[1]Veligaram Swetha
[2]Dr.A. Lakshmi Devi

Monte Carlo–Based EV Load Modelling and Optimal EVCS–DG Planning Using Pelican Optimization Algorithm

JES Journal of Electrical Systems

Abstract: - The stochastic nature of electric vehicles poses significant challenges to the radial distribution systems. In this paper, the electric vehicle load is modelled using a Monte Carlo Simulation (MCS) framework by considering key parameters such as initial state of charge, final state of charge, and charging start time. The peak EV demand obtained from the MCS analysis is considered as the electric vehicle charging station (EVCS) load, and three optimal EVCS locations are determined using a new optimization algorithm called the pelican optimization algorithm (POA). A multi-objective optimization problem is formulated and tested on the IEEE-69 and IEEE-85 bus radial distribution systems. Coordinated placement of three EVCSs with three types of distributed generation (Type-I, Type-II, and Type-III) is carried out and benchmarked against Particle Swarm Optimization (PSO). Turning to the result highlights, the MATLAB analysis reveals notable outcomes. Specifically, in the IEEE-69 bus system, power losses reduced by 97.93%, AVDI decreased to 0.000002 p.u, and the VSI increased to 0.976979 p.u. In the IEEE-85 bus system, losses reduced by 92.49% and AVDI decreased to 0. 000049 p. u. Meanwhile, VSI reached 0.939066 p.u. Furthermore, POA exhibits improved convergence behaviour and overall performance, highlighting its effectiveness for EV-integrated distribution network planning.

Keywords: Electric vehicle charging stations, Monte Carlo simulation, Pelican Optimization Algorithm, Particle Swarm Optimization

I. INTRODUCTION

The continuous growth of the global population has led to a significant increase in demand for transportation and electricity generation. Both sectors are heavily dependent on fossil fuels as their primary energy source, resulting in a surge in their consumption over recent decades [1]. According to studies presented in [2], production will rise by 54% in the transport industry by 2035, which will increase prices and air pollution due to significant demand
This causes fluctuations in energy prices and increases economic vulnerability, but also generates extensive greenhouse gas (GHG) emissions, particularly carbon dioxide (CO_2), which is the leading contributor to anthropogenic climate change.

Furthermore, continued reliance on fossil-based infrastructure undermines long-term energy security, as non-renewable resources are being exhausted at rates far exceeding their natural formation. In this regard, the promotion of electrified, low-carbon transportation systems—such as electric vehicles with integrated distributed energy generation technologies—has emerged as a promising strategy. These advancements not only contribute to emission reduction but also enhance the resilience and efficiency of modern energy systems.

Effective planning and operation are essential elements for minimizing operational risks associated with the utilization of existing distribution networks and accommodating a substantial number of EVs. To support a thorough study of distribution networks incorporating EV charging stations, modelling the charging loads related to electric vehicles (EVs) is an essential task. The majority of the research considered EV load as a constant power load, neglecting the inherent stochasticity associated with EV user behavior. In practice, EV charging demand is highly uncertain, depending on several random factors, including arrival and departure times, initial and final state of charge (SOC), charging duration, battery capacity, and charging power levels. The development of mathematical modelling of EV load patterns becomes a key aspect that allows scientists to conduct more realistic studies to forecast energy demand and propose solutions to problems that may arise [3]

Probabilistic load modelling methodologies utilising Monte Carlo Simulation (MCS) have garnered heightened interest in contemporary literature [4]. The EV load estimating process using MCS is conducted using several samples created from PDFs, depending on the input data. In [7], the demand for MCS EV charging is assessed, along with its effects on voltage profiles and line congestion in radial distribution networks [5]. In [6], spatio-temporal charging load curves are produced based on realistic user behaviour, whereas in [7], aggregated charging demand is predicted using advanced probabilistic methods

From a power system planning perspective, the stochastic increase in real and reactive power demand introduced by EV charging stations can significantly deteriorate voltage profiles and increase power losses, particularly in radial distribution systems. To alleviate these adverse impacts, the integration of distributed generators (DGs) has been widely recognized as an effective solution. Depending on their operational characteristics, DGs are generally classified as Type-1 (real power injection only), Type-2 (reactive power injection only), and Type-3 (supplies both real and reactive power) [8].

The majority of the studies have shown that the combined operation of EVCS and DGS has improved the voltage profile, real and reactive power loss reduction, feeder loading, voltage stability indices, and overall hosting capacity of distribution networks. The researchers in [9] used the grasshopper optimization algorithm (GOA) and introduced a two-stage fuzzy multi-objective

[1] *Research Scholar, Department of EEE, Sri Venkateswara University College of Engineering, India.
[2] Professor, Department of EEE, Sri Venkateswara University College of Engineering, India.

approach for optimal placement and sizing of DGs, shunt capacitors, and EVCSs. The objectives included loss minimization, voltage profile improvement, and cost reduction

In [10], the Political Optimization Algorithm (POA) is employed to optimally allocate renewable DGs and EVs with the objectives of real power loss minimization and voltage profile improvement. The authors in [11] investigated the optimal siting and sizing of EV charging stations and DGs using metaheuristic optimization techniques. Researchers in [12] proposed a competitive algorithm for the coordinated placement of DGs, capacitors, and EV charging stations, targeting loss minimization and voltage deviation reduction. In [13 metaheuristic-based multi-objective planning framework is presented for EVCSs and DGs, demonstrating that coordinated integration significantly enhances overall distribution system performance.

From the literature survey, we can observe that most studies addressing MCS-based EV load modelling do not jointly consider the optimal integration of DGs. Conversely, DG planning studies often assume deterministic or average EV loads, thereby neglecting the uncertainty inherent in real-world EV charging behaviour.

In this paper, an integrated planning framework is presented that combines Monte Carlo–based EV load modeling with the optimal placement and sizing of different DG types. A multi-objective function is developed to mitigate the average voltage deviation index and power losses, while enhancing the voltage stability index in distribution networks.

II. EV LOAD MODELLING

Load modelling of EV is highly stochastic, as it depends on many random factors, which must be quantified before calculating daily charging load profiles. Initial SOC, final SOC, and charging start time are some of the factors considered in this paper. The Monte Carlo simulation method is used to determine the probability distribution functions of parameters required for EV load modelling.

A. Initial state-of-charge (SOC): The initial soc is the SOC of the EV battery just before switching to the charging mode. The initial SOC may be influenced by variables such as the duration required for an electric vehicle (EV) user to travel to and from their workplace.

Figure 1 illustrates the initial battery State of Charge (SOC) distribution for charging events from The EV Project, which analysed 3,499 Nissan Leaf vehicles (October–December 2013) [14]. A beta distribution with shape parameters α = 3.28 and β = 3.27 effectively models this initial SOC distribution [15].

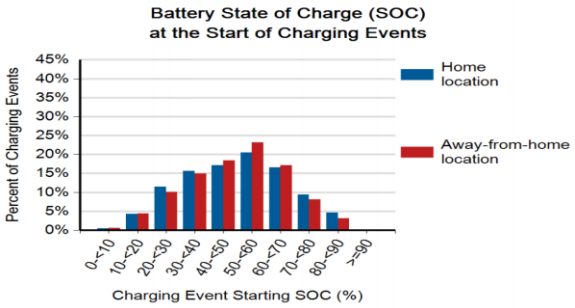

Figure 1: Initial Battery SOC Distribution from The EV Project [14].

The beta distribution [16], denoted Be (α, β) for positive scalars α and β, is a continuous probability distribution on [0, 1] whose probability density function is given as:

$$f(x) = \frac{x^{\alpha-1}(1-x)^{\beta-1}}{\text{Be}(\alpha,\beta),} \text{ for } 0 \leq x \leq 1 \quad (1)$$

$$\text{where, Be } (\alpha, \beta) = \int_0^1 x^{\alpha-1}(1-x)^{\beta-1}\ dx \quad (2)$$

A histogram of the initial SOC data from the EV Project, along with the fitted beta distribution, is shown in below figure 2

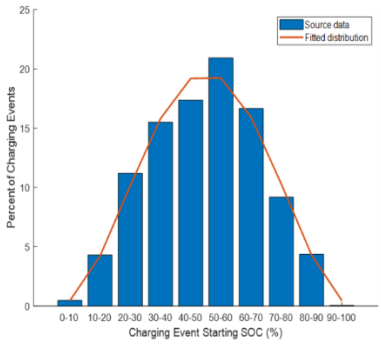

Figure 2: Initial SOC histogram with fitted beta pdf

B.Final State-Of-Charge: The final SOC could be due to a variety of reasons, such as their daily driving range, the rate of charging of their home charger, or the time at which charging begins.

Figure 3 illustrates the distribution of SOC after charging events for the same cohort of Nissan Leaf vehicles within the aforementioned reporting period. Generally, EV users tend to charge their cars to nearly full capacity before commencing their travels.

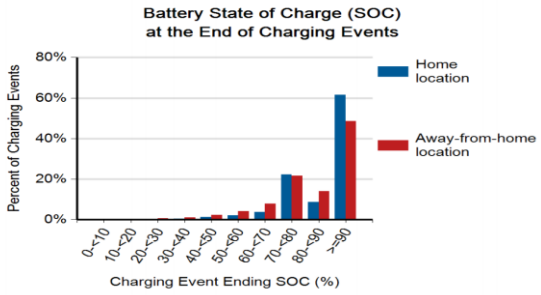

Figure 3: Final SOC distribution pack

The final SOC distribution is modeled in two segments: levels up to 80% are fitted with a beta distribution α = 5.51, β = 0.16, as shown in Figure 4; whereas the range from 80% to 100% is modeled by another beta distribution α = 14.59, β = 0.67, illustrated in Figure 5 [16].

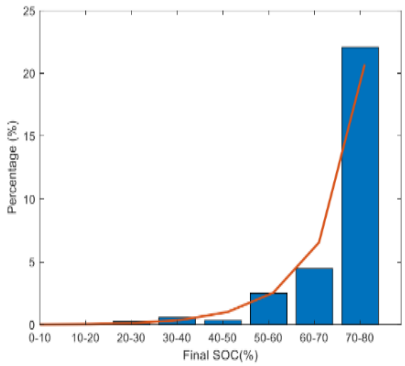

Figure 4: Final SOC with beta parameters α = 5.51 and β = 0.16

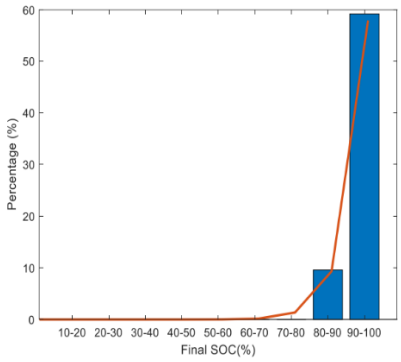

Figure 5: Final SOC with beta parameters α = 14.59 and β = 0.67

C.Charging Start Time: The start time for charging is inherently unpredictable and varies both daily and between individuals. However, when considered collectively, charging behaviour shows patterns that are suitable for probabilistic analysis modelling. This paper examines the start times of charging events data from 85 electric vehicles (EVs) collected between 2015 and 2017 in Texas, Colorado, and California [17]. Since no standard probability distributions fit the observed pattern, a custom probability density function is created.

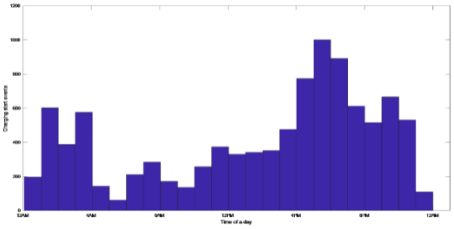

Figure 6: A histogram showing the sampled distribution of charging start time

D.Charging Duration Period: The charging duration can be obtained as

$$T_{c,n} = \frac{(SOC_f - SOC_i)CapEv_i}{P^C_{Evi} \times \eta} \quad \forall\, n \in N_e \qquad (3)$$

Where T_{Evi} represents the charging duration, SOC_f is the final SOC, SOC_i is the initial SOC, $CapEv_i$ is the battery capacity, P^C_{Evi} is the charging power, η is efficiency, N_e is the total No. of EVs

The total charging load P^{Ev}_{load} (t) is calculated by accumulating the charging power across all time periods, and is calculated as below.

$$P^{Ev}_{load}(t) = \sum_{n=1}^{Ne} P^{Ev}_{c,n}(t) \qquad (4)$$

Where $P^{Ev}_{c,n}(t)$ represents the charging power of the nth vehicle

E.Algorithm of MCS:

1. Set total EVs N and initialise n=1
2. Define Monte Carlo iterations M
3. Sample initial SOC, final SOC, and start time from their probability density functions.
4. Calculate the required charging demand and charging time
5. Record the nth Ev's load profile
6. Repeat for all EVs and sum individual profiles to get the total load curve.

Figure 7 shows the load profile of 1000 EVs computed using the Monte Carlo Simulation method

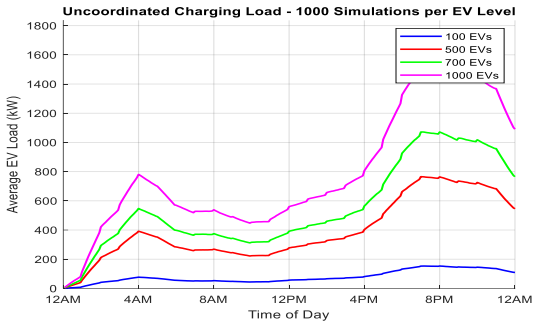

Figure 7: EV load calculated using Monte Carlo simulation

In this paper, we specifically examine the peak load of 1,000 EVs, which reaches 1,595 kW, to determine optimal locations of three EVCSs and to assess their impact on the distribution system.

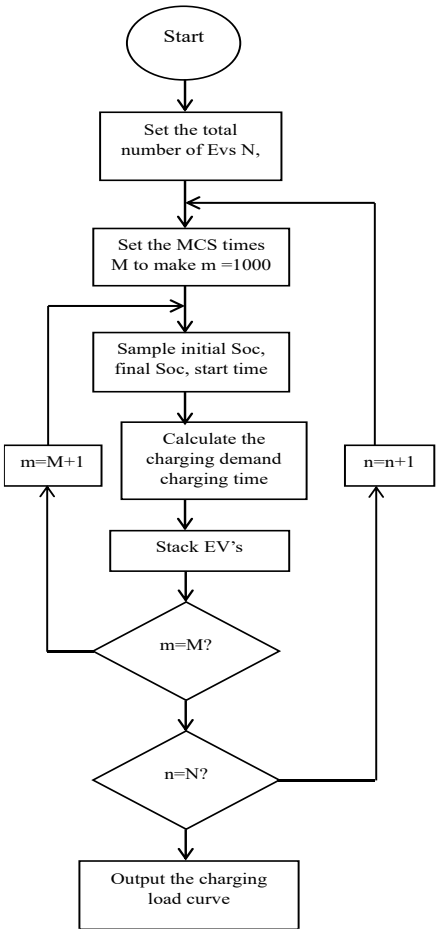

Figure 8: Flowchart of EV load calculation using Monte Carlo Simulation

III. PROBLEM FORMULATION

A. Load Flow

Conventional load flow studies, like Gauss-Seidel, Newton-Raphson, and Fast Decoupled load flow methods, are not suitable because of the high R/X ratio of distribution networks. Hence, the Direct Load Flow method is used for distribution networks, which gives better results. This load flow uses two matrices: bus injection to branch current matrix (BIBC) and bus current to bus voltage matrix (BCBV) matrices to calculate the power loss.

In the radial distribution system, the voltage at the k+1 bus is given as

$$V_{k+1} = V_k - I(R_{k,k+1} + j * X_{k,k+1}) \quad (5)$$

Here V_k, V_{k+1} , are the voltages at kth and (k+1) th buses. $R_{k,k+1}$, $X_{k,k+1}$) are the resistance and reactance, I is the branch current. The branch current I is calculated using bus injection to branch current matrix (BIBC) as

$$I=[BIBC]\ I \quad (6)$$

The current injected at the k+1 bus is given as,

$$i_{k+1} = \frac{(P_{k+1}+j*Q_{k+1})^*}{V_k} \quad (7)$$

Where P_{k+1}, Q_{k+1} are active and reactive power demands at bus k+1.
The power loss of the line section connecting buses k and k +1 may be computed as

$$P_{Loss}(k,k+1) = R_{k+1} * \left(\frac{P_k^2+Q_k^2}{|V_k^2|}\right) \quad (8)$$

$$Q_{Loss}(k,k+1) = X_{k+1} * \left(\frac{P_k^2+Q_k^2}{|V_k^2|}\right) \quad (9)$$

The total losses are obtained as below

$$P_{loss}^{Total} = \sum_{k=1}^{N} P_{Loss}(k,k+1) \quad (10)$$

$$Q_{loss}^{Total} = \sum_{k=1}^{N} Q_{Loss}(k,k+1) \quad (11)$$

B. Objective Function

The objective function of the paper is to minimize power loss, AVDI, and enhance VSI.

Active Power Loss: EVCSs impose substantial load demands, thereby increasing active power loss when they are placed at optimal nodes within the distribution network. Hence, the aim is to minimize the active power loss and is given as:

$$f_1(k) = \min \sum_{k=1}^{N_{br}} R_j * I_j^2 \quad (12)$$

Average Voltage Deviation Index: A node's voltage deviation index is the difference between the node's actual voltage and the reference voltage (1 p.u.) in a network. The AVDI represents the average VDI across all nodes in the network. A lower value signifies greater voltage stability, and it is given as

$$f_2(k) = \frac{1}{b} \sum_{k=1}^{b} |1 - V_k|^2 \quad (13)$$

Voltage Stability Index (VSI): The maximum Voltage Stability Index (VSI) of the distribution system indicates that the bus can maintain its voltage profile within acceptable limits, even under varying loading conditions. It is important to keep the VSI of all buses in the distribution system close to unity to ensure the safe operation of the system, and is given as

$$f_3(k) = |V_k|^4 - 4 * [P_{k+1}X_{j-} Q_{k+1} R_j]^2 - 4 * [P_{k+1}R_{j-} Q_{k+1} X_j] |V_k|^2 \quad (14)$$

In this study, three different objective functions are developed to (i) reduce the real power loss, (ii) minimize the Average Voltage Deviation Index (AVDI), and (iii) enhance the Voltage Stability Index (VSI). This multi-objective optimization problem is formulated using a weighted-sum approach and is expressed as:

$$F(k) = \min [w_1(f_1(k) + w_2(f_2(k) + w_3 \frac{1}{f3(k)} \quad (15)$$

where w1 accounts for 50% of the impact on power losses, w2 represents 20% of the effect on AVDI, and w3 reflects 30% of the influence on VSI.

C. Operational Constraints

Power balance constraints

$$P + P_{DGs} = P_{Load} + P_{Loss} + P_{Load}^{EVs} \quad (16)$$

Voltage Constraints

$$V_{min} \leq V_k \leq V_{max} \qquad K=1,2,3, \ldots\ldots N_{bus} \quad (17)$$

Power Limits of DGs

$$DG_{min} \leq DG_{Sizing} \leq DG_{max} \quad (18)$$

Where DG_{Sizing} limits are in kW, kVAR. kVA for Type I, II, and III DGS, respectively.

IV. Optimization Algorithms

A. Particle Optimization Algorithm

Particle Swarm Optimization is a metaheuristic approach, first introduced by Kennedy and Eberhart in 1995[18]. PSO is a population-based stochastic optimization algorithm that addresses various search and optimization challenges by mimicking the collective intelligence observed in natural swarms such as bird flocks and fish schools.

It works on a swarm of N particles in a search space with D dimensions. Each particle is a possible answer to an optimisation problem. Each particle progressively adjusts its position by incorporating its previous velocity vector, its individual optimal position (pbest), and the collective optimal position (gbest) disseminated throughout the swarm. [19]

Two fundamental equations govern particle dynamics in PSO. For particle *i,* the velocity and position updates are formulated as:

Velocity Update Equation:

$$V_i^{k+1} = \omega^k \times V_i^{k+1} + C_1 \times rand_1 \times (P_{best,i}^k - X_i^k) + C_2 \times rand_2 \times (G_{best,i}^k - X_i^k) \quad (19)$$

The inertia weight used is calculated using the equation

$$\omega^k = \omega_{max} - \left(\frac{\omega max - \omega min}{kmax}\right) \times k \quad (20)$$

Position Update Equation:

$$X_i^{k+1} = X_i^k + V_i^{k+1} \quad (21)$$

Where n represents the number of particles in the search space

Algorithm for PSO:

1. Initialize data, EVCS, and DG numbers.
2. Set the number of iterations and other parameters of PSO along with EVCSs and DG lower and upper bound limits.

3. Initialize the velocities and positions of the particle's population in the swarms.
4. Set the iteration to one.
5. Perform the load flow analysis and evaluate the best particle's index, velocities, position, and power losses.
6. Determine the Global optimum and Local optimum
7. According to Equations (28) and (30), update the velocities and locations.
8. The optimal value is assessed, and the optimal particle index for EVCS and DG is identified
9. Update the Gbest and Pbest of swarms.
10. Repeat steps 6–12, incrementing by 1, until the maximum number of iterations is attained.
11. Print the best solution and end.

B. Pelican Optimization Algorithm

The proposed algorithm, POA, is a nature-inspired metaheuristic introduced by Trojovský and Dehghani in 2022[20], drawing its inspiration from the cooperative hunting strategies employed by pelican colonies. These aquatic birds exhibit remarkable group coordination when pursuing prey, utilizing a two-stage approach: first identifying and approaching fish schools, then spreading their wings across the water surface to corral prey into their throat pouches. This hunting behaviour translates into a computational framework where pelicans represent candidate solutions that evolve through exploration and exploitation phases.

The algorithm's key advantage lies in its simplicity and derivative -free operation, making it suitable for non-differentiable, multimodal, and complex optimization landscapes. We present here the mathematical formulation and operational principles of this relatively recent addition to the family of swarm intelligence algorithms.

The initialization of the population is done by

$$X_{i,j} = l_j + \text{rand}.\,(u_j - l_j)\ ,\ i=1, 2,\ldots., N,\ j=1,2\ldots.m \tag{22}$$

Where X_(i,j) denotes the value of the jth variable as defined by the ith candidate solution, lj signifies the jth lower bound, and uj denotes the jth upper limit of the problem variable, rand is a random number in the interval [0, 1], N represents the number of population members, m indicates the number of problem variables

In this POA, the population of pelican agents is represented by a population matrix. Each row corresponds to a candidate solution vector, while each column denotes the recommended values for the decision variables

$$X=\begin{bmatrix} X_1 \\ \vdots \\ X_i \\ \vdots \\ X_N \end{bmatrix}_{N\times m} = \begin{bmatrix} x_{1,1} & \cdots & x_{1,j} & \cdots & x_{1,m} \\ \vdots & \vdots & \vdots & \vdots & \vdots \\ x_{i,1} & \cdots & x_{i,j} & \cdots & x_{i,m} \\ \vdots & \vdots & \vdots & \vdots & \vdots \\ x_{N,1} & \cdots & x_{N,j} & \cdots & x_{N,m} \end{bmatrix}_{N\times m} \tag{23}$$

where X is the population matrix, and Xi represents the ith individual pelican.

The above initial populations are used to determine the objective functions in the vector form, as shown below

$$F = \begin{bmatrix} F_1 \\ \vdots \\ F_i \\ \vdots \\ F_N \end{bmatrix}_{N\times 1} = \begin{bmatrix} F(X_1) \\ \vdots \\ F(X_i) \\ \vdots \\ F(X_N) \end{bmatrix}_{N\times 1} \tag{24}$$

The POA approach is represented in two phases based on pelicans' hunting behavior. The hunting behaviour is simulated using two phases

(i) Moving towards prey

Exploration entails moving toward the prey, whereas exploitation necessitates gliding on the water's surface. During the initial phase, pelicans randomly identify and approach their prey within the search space, mathematically represented by the equation

$$x_{i,j}^{p_1} = \begin{cases} x_{i,j} + \text{rand}.\,(p_j - l.\,x_{i,j}), & F_p^1 < F_i \\ x_{i,j} + \text{rand}.\,(x_{i,j} - p_j), & \text{else} \end{cases} \tag{25}$$

where Fp represents the prey objective function value.

A pelican agent's new position is accepted only if it yields a better objective function value. This effective updating criterion steers the algorithm away from suboptimal regions, avoiding premature convergence to local optima.

The position of the POA is updated using the equation below

$$X_i = \begin{cases} X_i^{P_1}, F_i^{P_1} < F_i\ ; \\ X_i\ , \text{else}\ , \end{cases} \tag{26}$$

(ii). Winging on the water surface

During this phase, pelicans use the surface of the water to push fish up by spreading their wings, thereby catching the fish in their throat bag. Pelicans capture a greater quantity of fish in the region targeted by this method. During this phase, the algorithm gets closer to finding better solutions in the hunting zone, which makes it easier to take advantage of POA. This pelican's hunting behaviour is written mathematically as

$$x_{i,j}^{p_2} = x_{i,j} + R.\,(1 - \frac{t}{T}).\,(2.\,\text{rand} - 1).\,x_{i,j} \tag{27}$$

Effective updating has been used to decide whether to accept or reject the most recent pelican position, as shown in the equation below.

$$X_i = \begin{cases} X_i^{P_2}, F_i^{P_2} < F_i ; \\ X_i , \text{else} , \end{cases} \quad (28)$$

Algorithm Procedure

1. Initialize the bus and line data, EVCS, and DG numbers.
2. Initialize the number of iterations and other parameters of POA along with EVCSs and DG lower and upper bound limits.
3. Randomly initialise the places of the pelican population inside the defined search space limits for EVCS sites and DG capacity.
4. Set the iteration counter t = 1.
5. Evaluate the fitness of each pelican using load flow analysis and other performance indices for the current EVCS and DG placement configuration.
6. Identify the global best position (x_best) representing the optimal EVCS and DG configuration with minimum power losses.
7. Generate a random prey position within the search space bounds.
8. Update positions using equations (22)-(28)
9. Run load flow analysis for all updated pelican positions to evaluate new fitness values.
10. Update the global best position if any pelican achieves better performance (lower power losses) than the current global best.
11. Check boundary constraints for EVCS locations (valid bus numbers) and DG capacities (within specified limits). Apply corrections if positions violate bounds.
12. Increment iteration counter: t = t + 1 and repeat steps 7-13, till the maximum number of iterations is attained
13. Print the best solution and end.

V. Results and Discussions

A. System Description

The first test system is the IEEE-69 bus distribution network, comprising 69 nodes and 68 branches, with a total real and reactive demand of 3,803.9 kW and 2,693.1 kVAr. It operates at 12.66 kV and 100 MVA.

The second test system is the IEEE-85 bus distribution network, comprising 85 nodes and 84 branches, with a total real and reactive demand of 2,570.28 kW and 2,622.08 kVAr. It operates at 11kV and 100 MVA.

Three different scenarios are addressed in this work on two IEEE systems to validate the methodology.

Scenario 1: Base case

Scenario 2: Optimal placement of three EVCSs

Scenario 3: Optimal placement of three EVCSs with three DGs of different types

B. Results of the IEEE-69 bus system

Scenario 1: Base case

With the load flow analysis on the first test system, the base case real power and reactive power losses are 224.8807kW and 102.64393 kVAr, respectively. The minimum voltage of 0.9092 p.u is obtained at bus 65, whereas the minimum VSI value is 0.683325 p.u, and the AVDI minimum is 0.001460 p.u

Scenario 2: Optimal placement of three EVCSs

Both the optimization algorithms, PSO and POA, identified the optimal locations for three EVCS as 2,28, 47 for the IEEE-69 bus. The power loss increased to 225.6047kW. Additionally, VSI is decreased to 0.68332 p.u. and AVDI is increased to 0.001463 p.u as given in Table 1.

Table 1: IEEE-69 bus system performance before and after placement of EVCS

	Locations	**Ploss(kW)**	**AVDI (p.u)**	**VSI (p.u)**	**Vmin (p.u)**
Load flow					
Base Case	-	224.9345	0.001460	0.683325	0.9092
Three EVCS					
PSO	2,28,47	225.6047	0.001463	0.68332	0.9091
POA	2,28,47	225.6047	0.001463	0.68332	0.9091

Scenario 3: Optimal placement of three EVCSs with Three Different Types of DGS

The performance of the distribution system with various types of distributed generation systems integrated with electric vehicle charging stations (EVCS) is evaluated. For Type-1 DG, which supplies only active power, real power losses are reduced to 68.93% and 69.05% using particle swarm optimization (PSO) and the pelican optimization algorithm (POA), respectively. Additionally, the minimum voltage (Vmin) increases to 0.9789 p.u. and 0.9790 p.u., while the voltage stability index (VSI) improves to 0.9182 p.u. and 0.9188 p.u. The average voltage deviation index (AVDI) values decrease to 0.000079 p.u. and 0.000076p.u.

For Type-2 DG, which provides only reactive power, real power losses are reduced to 32.04% and 32.32% with PSO and POA, respectively. Furthermore, the minimum voltage (Vmin) increases to 0.9305 p.u. and 0.9339 p.u., while the voltage

stability index (VSI) improves to 0.760689 p.u. and 0.765673 p.u. The average voltage deviation index (AVDI) values decrease to 0.000694p.u. and 0.000678 p.u.

In the case of a Type-3 DG that supplies both real and reactive power, there is a great reduction in real power losses of 97.38 % with PSO and 97.93 % with POA. The VSI reached 0.976944 p.u. and 0.976979 p.u.AVDI minimized to 0.000005 p.u., and 0.000002 p.u respectively. The minimum voltage has been improved to 0.9942 p.u with both optimisation procedures, as shown in Table 2.

Table 2: Performance Indices of IEEE-69 bus system

	Locations	Sizes	Ploss(kW)	% Reduction in Loss	AVDI (p.u)	VSI (p.u)	Vmin (p.u)
Type-I DG (kW)							
PSO	11	585	70.0875	68.93	0.000079	0.918202	0.9789
	61	1719					
	18	311					
POA	11	530	69.8192	69.05	0.000076	0.918788	0.9790
	17	380					
	61	1721					
Type-II DG (kVAr)							
PSO	11	1200	153.3084	32.04	0.000694	0.760689	0.9305
	17	381					
	61	1200					
POA	11	1000	152.6763	32.32	0.000678	0.765673	0.9339
	18	466					
	61	997					
Type-III DG (kVA)							
PSO	12	598+i185	5.9109	97.38	0.000005	0.976944	0.9942
	16	263+i198					
	61	1683+i187					
POA	11	498+i354	4.6751	97.93	0.000002	0.976979	0.9942
	18	379+i251					
	61	1675+i1195					

The voltage profile across various scenarios is depicted in the figure 8. It has been observed that the addition of EVCS has led to a degradation in the voltage profile. Therefore, distributed generation systems are incorporated to alleviate the effects on the voltage profile. It can be observed that while the voltage profile is improved with Type -2 distributed generation, it is still inferior to the other types of distributed generation. Therefore, it is not recommended. Conversely, the Type-3 dg exhibited an enhancement in the profile nearing unity, which made it the most suitable option for integration to minimise its impact on the voltage profile.

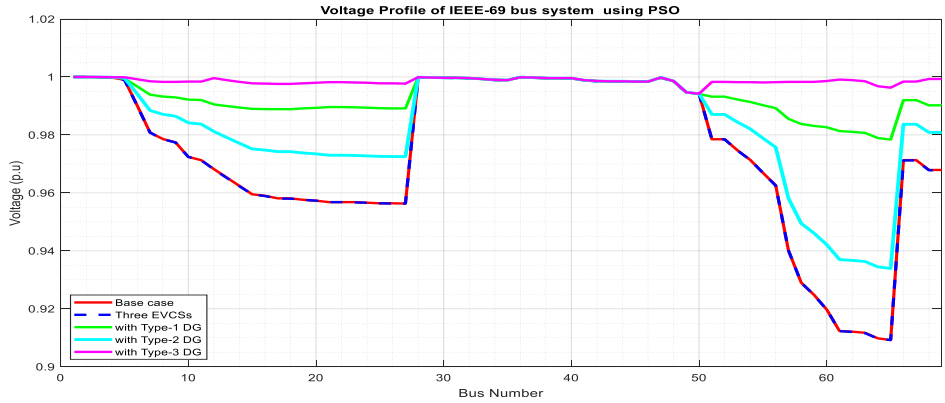

8a

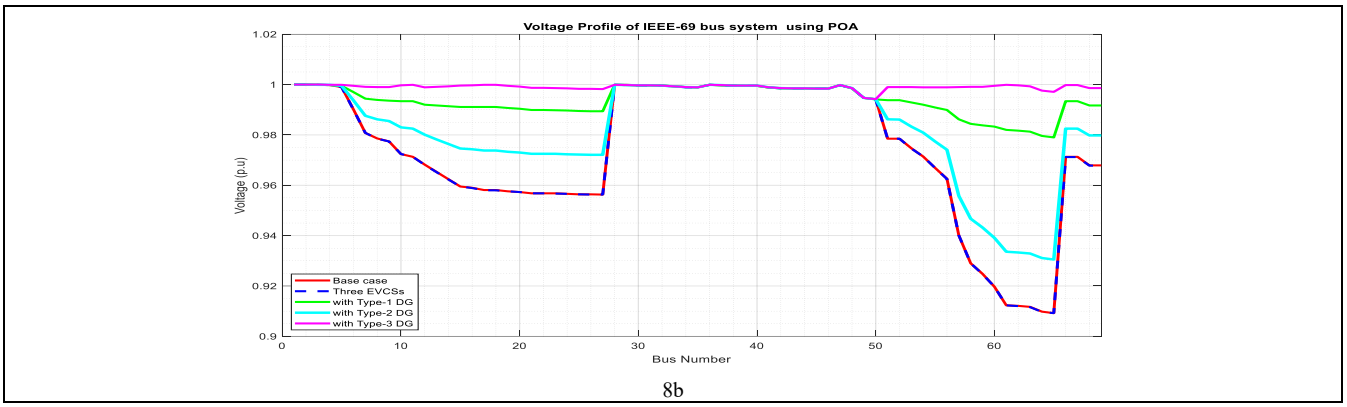

Figure 8: Voltage profiles of the IEEE-69 bus system, a) with PSO, b) with POA

The convergence curves of different scenarios are shown in the figure 9. Though PSO converges fast, POA yields better results.

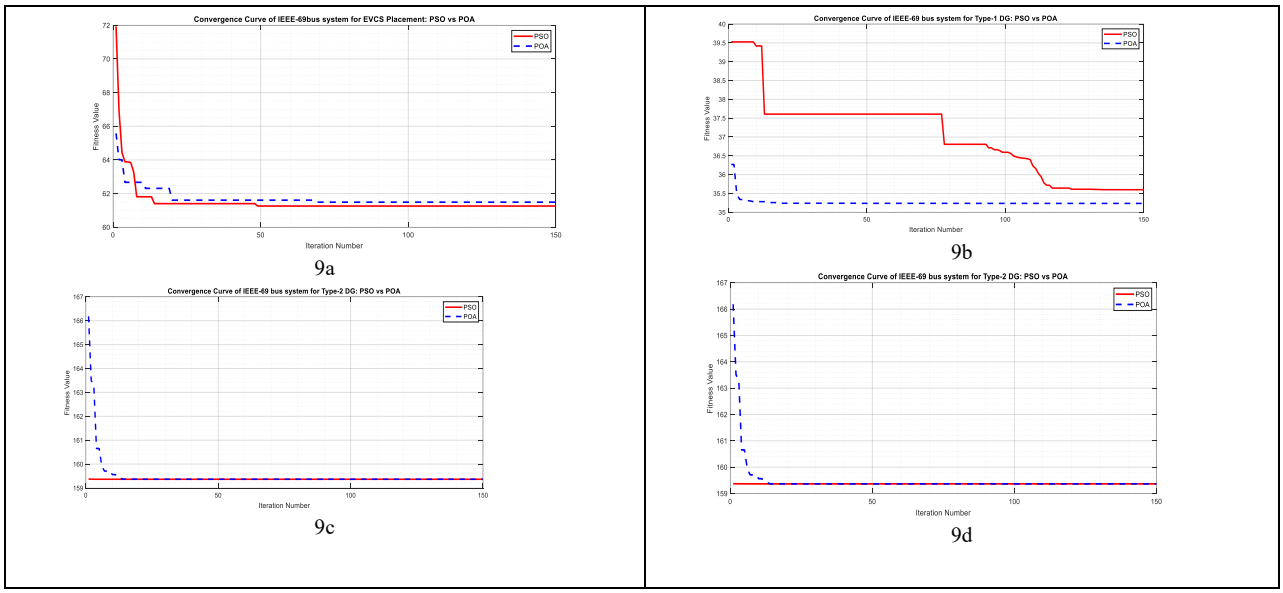

Figure 9: Convergence curves of the IEEE-69 bus system, a) with EVCS only, b) EVCS with Type-1 DG, c) EVCS with Type-2 DG d) EVCS with Type-3 DG

C. Results of the IEEE-85 bus system

Scenario 1: Base case

With the load flow analysis on the first test system, the base case real power and reactive power losses are 224.8807kW and 102.64393 kVAR, respectively. The minimum voltage of 0.9092 p.u is obtained at bus 65, whereas the minimum VSI value is 0.683325 p.u, and the AVDI minimum is 0.001460 p.u.

Scenario 2: Optimal Placement of Three EVCs.

Both the optimization algorithms, PSO and POA, identified the optimal locations for three EVCS as 2, 16, and 37 for the IEEE-85 bus. The power loss increased to 753.6750kW. Additionally, VSI is decreased to 0.4251 p.u. and AVDI is increased to 0.22365 p.u.

Table 3: IEEE-85 bus system performance before and after placement of EVCS

	Locations	**Ploss(kW)**	**AVDI (p.u)**	**VSI (p.u)**	**Vmin (p.u)**
Base case					
Load flow	-	316.1034	0.009778	0.576366	0.8713
With Three EVCSs					
PSO	2,16,37	753.6750	0.22365	0.4251	0.8074
POA	2,16,37	753.6750	0.22365	0.4251	0.8074

Scenario 3: Optimal placement of Three EVCs with Three Different Types of DGS

. With Type-1DG, real power losses are reduced to 74.64% and 74.77%, respectively, with PSO and POA. In addition, Vmin is increased to 0.9557 p. u,0.9539 p.u, while the VSI improved to 0.834240 p.u, 0.828124 p.u., and the AVDI values reduced to 0.001300 p.u., 0.001448 p.u.

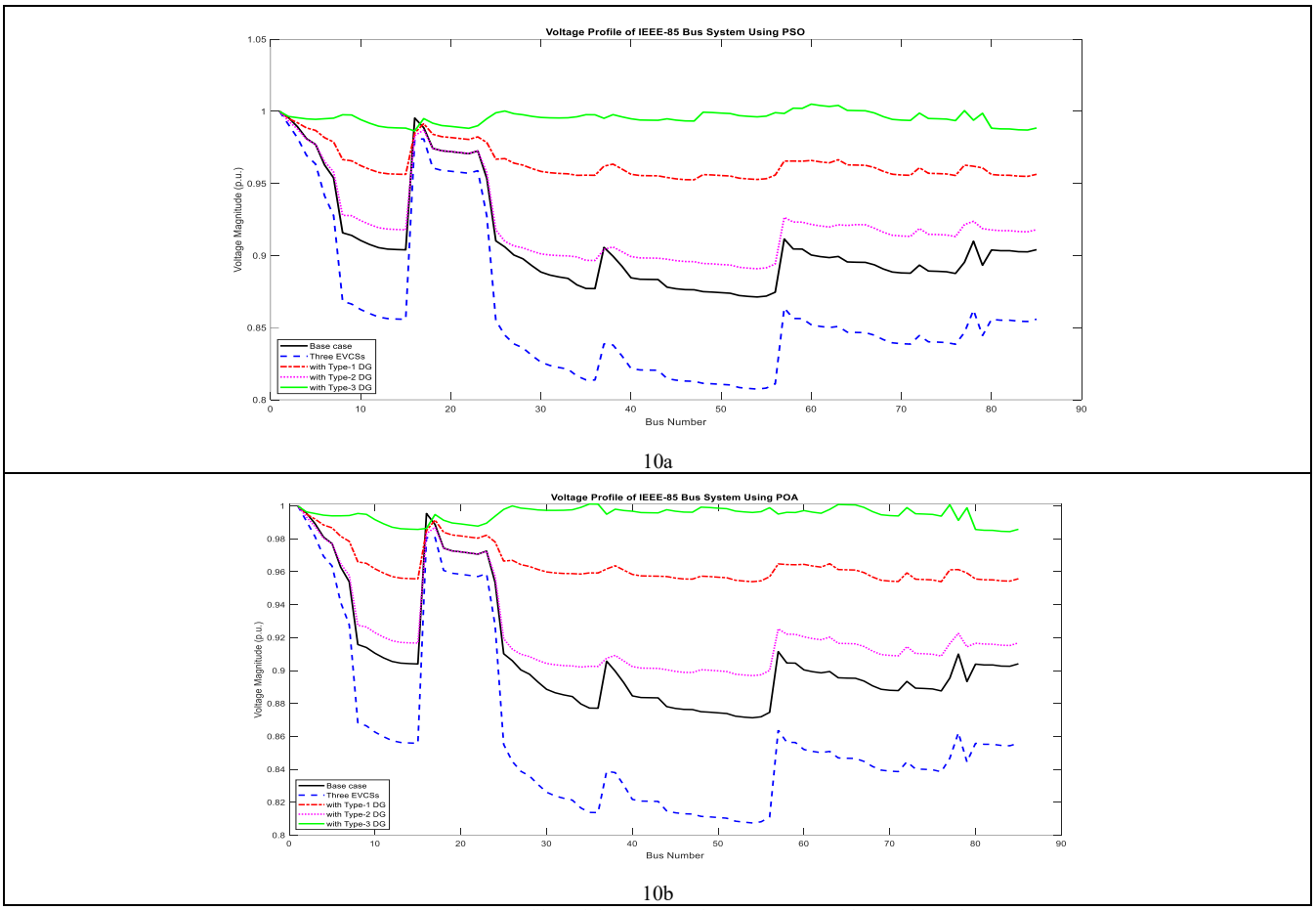

Figure 10: Voltage profiles of the IEEE-85 bus system, a) with PSO b) with POA

In the case of Type-2 DG, real power losses reduction is of 16.23% and 20.27%, respectively, when utilising PSO and POA. Furthermore, Vmin has risen to 0.9012 p.u and 0.8969 p.u, while the VSI has improved to 0.659735p.u and 0.647030p.u. The AVDI values have decreased 0.006668p.u and 0.006790p.u.

Table 4: Performance Indices of IEEE-85 bus system

	Locations	**Sizes**	**Ploss(kW)**	**% Reduction in Ploss**	**AVDI (p.u)**	**VSI (p.u)**	**Vmin (p.u)**
Type-1 DG (kW)							
PSO	26	2806	191.0923	74.64	0.001300	0.834240	0.9557
	35	539					
	64	634					
POA	26	2495	190.1649	74.77	0.001448	0.828124	0.9539
	35	547					
	63	861					
Type-2 DG (kVAr)							
PSO	60	1200	631.3418	16.23	0.006668	0.659735	0.9012
	28	1200					
	48	1200					
POA	26	1200	600.9281	20.27	0.006790	0.647030	0.8969
	35	1200					
	63	1200					
Type-3 DG (kVA)							
PSO	26	2370+i1070	58.1557	92.28	0.000070	0.939024	0.9844
	49	556+i417					
	60	824+i618					
POA	35	610+i457	56.6182	92.49	0.000049	0.939066	0.9844
	64	815+i611					
	26	2360+i984					

The results in Table 4 show that Type-3 DG achieves the highest loss reduction, at 92.28% using PSO, followed closely by 92.49% with POA. The minimum voltage is the same for both, which is 0.9844p.u.

While PSO demonstrated superior performance regarding VSI and Vmin, POA showed overall enhanced performance. The resulting convergence curves are illustrated in the figure. The voltage profiles with both optimization algorithms are illustrated in the figure 10. From the convergence curves shown in figure11, we can conclude that POA gives better fitness values.

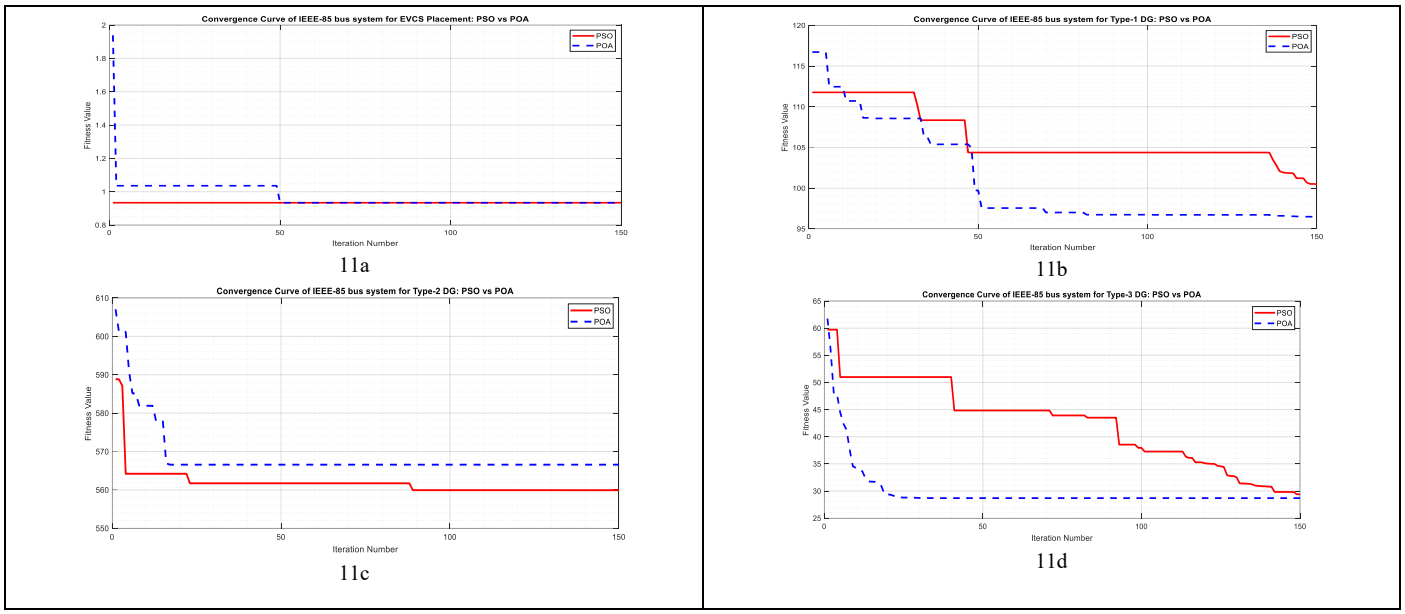

Figure 11: Convergence curves of the IEEE-85 bus system, a) with EVCS only, b) EVCS with Type-1 DG, c) EVCS with Type-2 DG, d) EVCS with Type-3 DG

VI. CONCLUSION

This study investigated the optimal placement of three electric vehicle charging stations (EVCSs) integrated with three different types of distributed generation (DG) units in radial distribution networks, employing Particle Swarm Optimization (PSO) and the recently proposed Pelican Optimization Algorithm (POA). The effectiveness of the proposed approaches was tested on the standard IEEE 69-bus and IEEE 85-bus test systems, considering the multi-objective function of minimizing power loss, AVDI, and enhancing VSI.

The results from both test systems unequivocally demonstrate the superior performance of Type-III DG units, which are capable of injecting both active and reactive power. In the IEEE 69-bus system, integrating Type-III DG resulted in a 97.38% reduction in active power loss with PSO and a 97.93% reduction with POA. Similarly, in the IEEE-85 bus system, integrating Type-III DG resulted in loss reductions exceeding 92% with both optimization techniques, also minimizing AVDI and enhancing VSI are obtained.

In summary, the results affirm that the coordinated placement of EVCSs alongside appropriately selected DG technologies—optimized via advanced metaheuristics such as POA—can substantially improve the technical performance of radial distribution systems. Overall, the findings confirmed the superior performance of the new metaheuristic technique, POA, making it suitable for future large-scale, multi-objective planning studies involving high penetration of electric vehicles and distributed energy resources

REFERENCES

1. F. Fazelpour, M. Vafaeipour, O. Rahbari, and M. A. Rosen, “Intelligent optimization to integrate a plug-in hybrid electric vehicle smart parking lot with renewable energy resources and enhance grid characteristics,” Energy Conversion and Management, vol. 77, pp. 250–261, January 2014, doi: 10.1016/j.enconman.2013.09.006.
2. F. Ahmad, A. Iqbal, I. Ashraf, M. Marzband, and I. Khan, “Optimal location of electric vehicle charging station and its impact on distribution network: A review,” Energy Reports, vol. 8, pp. 2314–2333, Nov. 2022. doi: 10.1016/j.egyr.2022.01.18.
3. 3 Huang, X.; Wu, D.; Boulet, B. Ensemble learning for charging load forecasting of electric vehicle charging stations. In Proceedings of the 2020 IEEE Electric Power and Energy Conference (EPEC), Edmonton, AB, Canada, 9–10 November 2020; pp. 1–5.
4. Bian, H.; Guo, Z.; Zhou, C.; Wang, X.; Peng, S.; Zhang, X. Research on orderly charge and discharge strategy of EV based on QPSO algorithm. IEEE Access 2022, 10, 66430–66448.
5. J. James and J. E. A., “Stochastic modeling of electric vehicle charging and impacts on the grid,” *Electric Power Systems Research*, vol. 246, 2025.
6. A. S. Khodayar *et al.*, “A stochastic methodology for EV fast-charging load curve estimation considering user behavior,” *Energies*, vol. 17, no. 7, 2024.
7. Y. Zhang *et al.*, “EV charging load forecasting using enhanced Monte Carlo simulation,” *Zhejiang Dianli*, 2025.

8. H. Pradeepa, T. Ananthapadmanabha, S. Rani D N, C. Bandhavya, Optimal allocation of combined DG and capacitor units for voltage stability enhancement, Procedia Technol. 21 (2015) 216–223, https://doi.org/10.1016/j. protcy.2015.10.091.
9. B. R. C. Grasshopper optimization algorithm-based two-stage fuzzy Mult objective approach for optimum sizing and placement of distributed generations, shunt capacitors and electric vehicle charging stations. J. Energy Storage. 27, 101117 (2020).
10. 10. Dharavat, N. et al. Sep., 'Optimal Allocation of Renewable Distributed Generators and Electric Vehicles in a Distribution System Using the Political Optimization Algorithm', Energies (Basel), vol. 15, no. 18, doi: (2022). https://doi.org/10.3390/en15186698
11. 11. Golive, S. G., Paramasivam, B., Ravindra, J. & 'INTELLIGENT SYSTEMS AND APPLICATIONS IN ENGINEERING Optimal. Siting and Sizing of Electric Vehicle Charging Stations and Distributed Generators in Distribution Systems by Meta Heuristic Techniques, vol. 12, pp. 55–62, (2024).
12. 12. Wang, S., Li, Z. & Golkar, M. J. 'Optimum placement of distributed generation resources, capacitors and charging stations with a developed competitive algorithm', Heliyon, vol. 10, no. 4, p. e26194, doi: (2024). https://doi.org/10.1016/j.heliyon.2024.e26194
13. 13. Mehroliya, S. & Arya, A. Optimal planning of power distribution system employing electric vehicle charging stations and distributed generators using metaheuristic algorithm. Electr. Eng. https://doi.org/10.1007/s00202-023-02198-3 (2024).
14. "EV Project Nissan Leaf Vehicle Summary Report," INL, ID, U.S., Rep. INL/MIS-11-21904, October 2019[Online], Available: https://avt.inl.gov/sites/default/files/pdf/EVProj/EVProjectNissanLeafQ42013.pdf
15. Alvarez Guerrero, J.D., Bhattarai, B., Shrestha, R., Acker, T.L. and Castro, R., 2021. Integrating electric vehicles into power system operation production cost models. *World Electric Vehicle Journal*, *12*(4), p.263.
16. Weisstein, E.W. *Beta Distribution*; MathWorld, Wolfram Web Resource. Available online: https://mathworld.wolfram.com/BetaDistribution.html
17. Bhattarai, B. Aggregator Based Charging Management of Electric Vehicles. Master's Thesis, Northern Arizona University, Flagstaff, AZ, USA, 2019. Available online: https://www.proquest.com/docview/2377906639?pq-origsite=primo
18. M. R. Mozafar, M. H. Moradi, and M. H. Amini, "A simultaneous approach for optimal allocation of renewable energy sources and electric vehicle charging stations in smart grids based on improved GA-PSO algorithm," Sustainable Cities and Society, vol. 32, pp. 627-637, Jul. 2017.
19. G. Battapothula, C. Yammani, and S. Maheswarapu, "Multi-objective simultaneous optimal planning of electrical vehicle fast charging stations and DGs in distribution system," Journal of Modern Power Systems and Clean Energy, vol. 7, no. 4, pp. 923-934, Jul. 2019.